Neurobiology of Disease

Innocuous, Not Noxious, Input Activates PKCγ Interneurons of the Spinal Dorsal Horn via Myelinated Afferent Fibers

Simona Neumann,[1,2] Joao M. Braz,[1,2] Kate Skinner,[1,2] Ida J. Llewellyn-Smith,[3] and Allan I. Basbaum[1,2]

Departments of [1]Anatomy and [2]Physiology and W. M. Keck Foundation Center for Integrative Neuroscience, University of California, San Francisco, San Francisco, California 94158, and [3]Cardiovascular Medicine and Center for Neuroscience, Flinders University, Bedford Park, South Australia 5042, Australia

Protein kinase C γ (PKCγ), which is concentrated in interneurons of the inner part of lamina II of the dorsal horn, has been implicated in injury-induced allodynia, a condition wherein pain is produced by innocuous stimuli. Although it is generally assumed that these interneurons receive input from the nonpeptidergic, IB4-positive subset of nociceptors, the fact that PKCγ cells do not express Fos in response to noxious stimulation suggests otherwise. Here, we demonstrate that the terminal field of the nonpeptidergic population of nociceptors, in fact, lies dorsal to that of PKCγ interneurons. There was also no overlap between the PKCγ-expressing interneurons and the transganglionic tracer wheat germ agglutinin which, after sciatic nerve injection, labels all unmyelinated nociceptors. However, transganglionic transport of the β-subunit of cholera toxin, which marks the medium-diameter and large-diameter myelinated afferents that transmit non-noxious information, revealed extensive overlap with the layer of PKCγ interneurons. Furthermore, expression of a transneuronal tracer in myelinated afferents resulted in labeling of PKCγ interneurons. Light and electron microscopic double labeling further showed that the VGLUT1 subtype of vesicular glutamate transmitter, which is expressed in myelinated afferents, marks synapses that are presynaptic to the PKCγ interneurons. Finally, we demonstrate that a continuous non-noxious input, generated by walking on a rotarod, induces Fos in the PKCγ interneurons. These results establish that PKCγ interneurons are activated by myelinated afferents that respond to innocuous stimuli, which suggests that injury-induced mechanical allodynia is transmitted through a circuit that involves PKCγ interneurons and non-nociceptive, VGLUT1-expressing myelinated primary afferents.

Key words: **PKCγ; pain; myelinated terminals; spinal cord; sensory neurons; CTB**

Introduction

There is now considerable evidence for a major contribution of the signal transduction enzyme protein kinase C (PKC) to the induction and maintenance of persistent pain after tissue or nerve injury. PKC acts in part through spinal cord circuits that transmit "pain" messages. Of particular interest is our previous report that mice with a targeted deletion of the gene that encodes PKCγ which, in contrast to the widely distributed α, βI, and βII isoenzymes, is restricted to a subpopulation of interneurons in the inner part of lamina II (IIi) of the superficial dorsal horn, show normal acute pain responses in the absence of tissue or nerve injury but, in the setting of injury, exhibit a significant decrease in pain behaviors in response to innocuous stimuli (allodynia) (Malmberg et al., 1997).

Unclear, however, are the anatomical links through which primary afferent nociceptors engage the PKCγ interneurons. Nociceptors are generally divided into two main classes (Snider and McMahon, 1998). The peptidergic [substance P and calcitonin-gene-related peptide (CGRP)] population terminates in superficial lamina I and outer lamina II (IIo) of the dorsal horn. The IB4, nonpeptidergic population targets inner lamina II. Based on what appeared to be a selective targeting of the PKCγ interneurons by the nonpeptidergic, IB4 subpopulation of nociceptors, we postulated that loss of injury-induced allodynia in the mutant mice resulted from functional disruption of a circuit involving these afferents, the PKCγ interneurons, and dorsal horn "pain transmission" neurons (Malmberg et al., 1997).

Recent data, however, suggest that the definition of inner lamina II, which contains the PKCγ interneurons and the IB4 terminals, needs revision. For example, a detailed analysis of the patterns of projection of IB4 afferents and of the MrgD subset of these afferents in the mouse showed that the latter terminate immediately dorsal to, rather than overlapping with, the band of PKCγ interneurons (Zylka et al., 2005). Furthermore, using a transneuronal tracing method to study the central connections of the IB4 afferents, we never found labeling of PKCγ interneurons, indicating that the latter are neither contacted by the IB4 afferents nor part of the spinal cord circuits engaged by them (Braz et al., 2005). It appears that lamina IIi is itself stratified, with a dorsal band that is targeted by IB4 afferents and a ventral band containing the PKCγ interneurons.

Here, we sought to identify the nature of the primary afferent input to the PKCγ interneurons. We first established that unmyelinated afferents, in fact, do not target these cells. In contrast,

Received Jan. 2, 2008; revised June 20, 2008; accepted June 23, 2008.

This work was supported by National Institutes of Health Grants NS48499 and NS14627, the Roman Reed Spinal Cord Injury Research Grant of California, National Health and Medical Research Council of Australia Project Grant 229907, and Research Fellowship 229921. We thank Carolyn Martin and Lee Travis for technical assistance.

Correspondence should be addressed to Simona Neumann, Department of Anatomy, University California, San Francisco, Rock Hall, Mission Bay, 1550 4th Street, San Francisco, CA 94158. E-mail: neumann@phy.ucsf.edu.

DOI:10.1523/JNEUROSCI.1259-08.2008

 0270-6474/08/287936-09$15.00/0

using a new transneuronal tracing method, we demonstrate that at least part of the primary afferent input to the PKCγ interneurons derives from myelinated primary afferent fibers. Next, we show that the vesicular glutamate transporter, VGLUT1, which is expressed by myelinated afferents, marks synapses presynaptic to PKCγ interneurons. Finally, we used Fos expression and find that innocuous inputs generated while walking on a rotarod activate the PKCγ interneurons. Our results raise the possibility that these interneurons are normally activated by nonpainful stimulation and that this circuit contributes to the mechanical allodynia that occurs in the setting of injury.

Materials and Methods

Animals. Sprague Dawley rats (200–250 g) or wild-type mice were purchased from Charles River or from the Animal House at Flinders Medical Centre. Transneuronal tracing was performed in double-transgenic mice in which transneuronal anterograde transport of the tracer wheat germ agglutinin (WGA) can be triggered in large-diameter primary afferents after transection of the sciatic nerve (J. M. Braz, unpublished results). These "NPY-ZW2" mice were generated by crossing our ZW2 line (Braz et al., 2002) with mice that express Cre recombinase in neuropeptide Y-positive neurons (DeFalco et al., 2001) (gift from Dr. J. M. Friedman, Rockefeller University, New York, NY). All animal experiments were reviewed and approved by the Institutional Animal Care Committee of the University of California, San Francisco or the Animal Welfare Committee of Flinders University.

Transganglionic tracing. Adult Sprague Dawley rats (200–250 g) or wild-type mice were anesthetized with isoflurane. Through a skin incision, the left sciatic nerve was exposed by blunt dissection. Next, the needle of a 10 μl Hamilton syringe or a glass pipette attached to a syringe was inserted through an epineurial incision and 1–1.5 μl of cholera toxin β subunit (CTB) conjugated to horseradish peroxidase (HRP) (CTB-HRP; List Biological Laboratories; 1% in distilled water), 3.0 μl of unconjugated CTB (List Biological Laboratories; 0.5% in distilled water), or 1.5 μl of WGA (Sigma; 5% in distilled water) was injected into the right sciatic nerve. Four to five days after tracer injection, the mice and rats were deeply anesthetized with pentobarbital (100 mg/kg) and perfused as described below.

Axotomy. NPY-ZW2 mice were anesthetized by an intraperitoneal injection of ketamine (60 mg/kg)/xylazine (8.0 mg/kg). To transect the sciatic nerve, we made an incision on the lateral aspect of the midthigh. The sciatic nerve was exposed and cut, and ~2.0 mm of the distal part of the nerve was removed. The overlying muscle and skin were sutured, and the mice were allowed to recover and then returned to their home cages.

Formalin-induced Fos expression. As a noxious stimulus, we injected formalin into the plantar surface of one hindpaw, in both rats (5%;100 μl) and mice (2%;10 μl). Ninety minutes after the formalin injection, the animals were anesthetized and perfused, and then the L4 and L5 lumbar spinal cord segments were processed for Fos and PKCγ immunoreactivity.

Rotarod assay. To induce Fos by non-noxious stimulation, we trained rats to walk on a rotarod and compared Fos expression in these animals with that in untrained, control rats. The experimental group of rats received one training session on the rotarod (lasting 1.5 h), 1 week before the trial. On the day of the experiment, the rats were placed on the rotarod for 1.5 h, after which time they were immediately anesthetized with pentobarbital (100 mg/kg, i.p.) and perfused for subsequent immunocytochemical colocalization of Fos and PKCγ (see below). We compared the percentage of cells double labeled for Fos/PKCγ in rats that had walked on the rotarod ($n = 4$) with results from control rats that remained in their cages ($n = 3$).

Tissue preparation. For light microscopic immunocytochemistry, the mice and rats were deeply anesthetized with pentobarbital (100 mg/kg, i.p.) and perfused with a 10% phosphate-buffered formalin fixative. After perfusion, the spinal cords were removed and postfixed in the same fixative (4 h for fluorescent labeling, 3 d for peroxidase labeling) and then cryoprotected in sucrose for a minimum of 10 h. The spinal cords were sectioned transversely (30 μm for immunofluorescence; 25 μm for immunoperoxidase) on a cryostat. Unless otherwise stated, 20 sections per animal from lumbar segments L4–L5 were used for these experiments.

For electron microscopic (EM) immunocytochemistry, rats were anesthetized with pentobarbital, flushed with oxygenated tissue culture medium (DMEM-F12; Sigma D-8900), and then perfused with 4% formaldehyde plus 0.3% glutaraldehyde in 0.1 M phosphate buffer, pH 7.4. Spinal cords were removed and postfixed overnight at 4°C in the same fixative. Cervical spinal cord segments C6–C8 and lumbar segments L3–L5 were embedded together in albumin gelatin (Alvarez et al., 2004; Llewellyn-Smith et al., 2007) and cut transversely at 50 μm on a Vibratome.

Light microscopic immunocytochemistry. We used double-immunofluorescence labeling to study the relationship between the distribution of PKCγ interneurons (Strategic Biosolutions; 1:5000) and primary afferent terminals, using antibodies directed against a variety of markers, including CGRP (Peninsula; 1:1000), IB4 (Sigma; 1:100), and VGLUT1 (Synaptic Systems; 1:1000). We also used double-immunofluorescence staining to study the relationship of the PKCγ neurons to terminals of unmyelinated primary afferents marked with a transganglionic tracer, WGA (Sigma; 1:50,000), or to the pattern of spinal cord Fos expression (1:5000) after noxious stimulation (hindpaw injection of formalin). In addition, in the double-transgenic NPY-ZW2 mice, we monitored expression of the WGA transgene using the antibody directed against WGA and a second that immunolabels dorsal root ganglion (DRG) neurons with myelinated axons (mouse anti-N52; Sigma; 1:10,000). The transneuronal transport of the WGA to PKCγ interneurons was demonstrated by double-immunofluorescence labeling for WGA and PKCγ.

Transverse sections of rat as well as mouse spinal cords were preincubated for 30 min in PBS containing 0.5% Triton X-100 and 10% normal goat serum (NPBST) and then immunostained overnight in the same buffer containing primary antibodies. After washing in NPBST, sections were incubated in a secondary antibody conjugated to Alexa 568 or Alexa 488 (Invitrogen; 1:700) for 1 h. All incubations were done at room temperature. Immunostained sections were mounted and coverslipped with Fluoromount-G (Southern Biotech). Double-immunoperoxidase labeling was used in experiments to localize PKCγ plus VGLUT1 or CTB and for studies of Fos expression in PKCγ interneurons after rotarod walking.

Before exposure to anti-VGLUT1, transverse sections through C6–C8 and L3–L5 were washed three times for 10 min each in 10 mM Tris, 0.9% NaCl, 0.05% thimerosal in 10 mM sodium phosphate buffer, pH 7.4 (TPBS) containing 0.03% Triton X-100 (Y-Triton), which was the diluent for all immunoreagents. Primary antibody solutions contained 10% heat-inactivated normal horse serum (NHS; Invitrogen), and secondary antibody solutions contained 1% NHS. After blocking in 10% NHS for 30 min, sections were incubated for 2–3 d in rabbit anti-VGLUT1 (Synaptic Systems; 1:5000) or in goat anti-CTB (List Biological Laboratories; 1:100,000) overnight in biotinylated donkey anti-Ig (Jackson ImmunoResearch Laboratories; 1:500) and then for 4–6 h in ExtrAvidin-peroxidase (catalog #E-2886; Sigma; 1:1500). Incubations were done at room temperature, and sections were washed three times for 10 min each in TPBS between incubations. VGLUT1-immunoreactive axons were revealed with a nickel-intensified diaminobenzidine (DAB) reaction (Llewellyn-Smith et al., 2005). After reexposure to 10% NHS, sections were incubated for 2–3 d in guinea pig anti-PKCγ (1:10,000; Strategic Biosolutions) and overnight in biotinylated donkey anti-guinea-pig Ig (Jackson ImmunoResearch; 1:500) and ExtrAvidin-peroxidase (Sigma; 1:1500). An imidazole-intensified DAB reaction (Llewellyn-Smith et al., 2005) revealed the PKCγ-containing interneurons, and then the sections were mounted and coverslipped with Permaslip (Alban Scientific).

For studies of Fos expression in PKCγ interneurons after rotarod walking, sections were first incubated overnight at 4°C in a 1:50,000 dilution of Fos protein antiserum (Oncogene). Immunostaining was performed according to the avidin–biotin peroxidase method (Hsu et al., 1981) using a nickel-intensified diaminobenzidine protocol with glucose oxidase to produce a black reaction product denoting nuclear Fos immunoreactivity. The sections were then incubated overnight in a 1:50,000 dilution of PKCγ antibody (Strategic Biosolutions) followed by the avi-

din–biotin peroxidase method without nickel, resulting in light brown, cytoplasmic PKCγ immunoreactivity. Reacted sections were mounted on gelatin-coated slides, dried, dehydrated, and coverslipped with DPX.

Electron microscopic immunocytochemistry. Transverse sections for electron microscopy were treated with 50% ethanol for 3 h (Llewellyn-Smith and Minson, 1992) to improve antibody penetration and then incubated in 10% NHS-TPBS for at least 30 min. Sections were first processed to reveal PKCγ-immunoreactive interneurons by incubation in guinea-pig anti-PKCγ diluted 1:20,000 in 10% NHS in TPBS, in biotinylated donkey anti-guinea-pig Ig (Jackson ImmunoResearch) diluted 1:500 in 1% NHS-TPBS, and finally in ExtrAvidin-peroxidase (Sigma) diluted 1:1500 in TPBS. Triton was not added to the diluents; all incubations were for 3 d, and sections were washed three times for 30 min each in TPBS between incubations. After the final wash, PKCγ immunoreactivity was visualized with a tetramethylbenzidine (TMB)–tungstate reaction in which peroxide was generated by glucose oxidase (Llewellyn-Smith et al., 1993) and the TMB–tungstate crystals were stabilized (Llewellyn-Smith et al., 2007). After another exposure to 10% NHS-TPBS, the sections were incubated in 1:75,000 rabbit anti-VGLUT1 (Synaptic Systems), in 1:500 biotinylated donkey anti-rabbit Ig (Jackson ImmunoResearch), and then in 1:1500 ExtrAvidin-peroxidase (Sigma). Incubations were for 3–5 d at room temperature. The specificity of the anti-VGLUT1 antibody has been confirmed (Llewellyn-Smith et al., 2007). Axons with VGLUT1 immunoreactivity were revealed with an imidazole-intensified DAB reaction (Llewellyn-Smith et al., 2005). After the second staining cycle, the sections were osmicated, stained *en bloc* with uranyl acetate, and processed into resin (Llewellyn-Smith et al., 2007). Ultrathin sections through regions of the dorsal horn that contained PKCγ interneurons were cut with a diamond knife, mounted on mesh or single slot grids, and stained with lead citrate for viewing with a JEOL 1200EX electron microscope.

Data and statistical analysis. To quantify the number of Fos-like immunoreactive neurons and the number of double-labeled Fos/PKCγ neurons, we used a Nikon microscope to photograph 15–25 sections (30 μm) from the L4–L5 spinal cord. We counted the total number of Fos-immunoreactive neurons, as well as the double-labeled Fos/PKCγ neurons in laminae IIi–III, where PKCγ neurons are concentrated. From the double-labeled Fos/PKCγ neurons and the total number of Fos-IR neurons, we generated a percentage value for Fos/PKCγ immunoreactive neurons per rat. Statistical significance was determined by Student's *t* test.

Results

Segregation of the CGRP- and IB4-positive terminals from the PKCγ interneurons

As noted above, peptidergic sensory neurons project predominantly to laminae I and IIo of the superficial dorsal horn (McNeill et al., 1988; Snider and McMahon, 1998); the nonpeptidergic IB4-positive neurons project to IIi (Silverman and Kruger, 1990; Snider and McMahon, 1998; Hunt and Mantyh, 2001). The PKCγ interneurons are also concentrated in inner lamina II (Mori et al., 1990; Malmberg et al., 1997; Polgár et al., 1999). As expected, therefore, double labeling of spinal cord sections with CGRP and PKCγ antibodies showed that there is no overlap in the distribution of CGRP-immunoreactive terminals and the PKCγ interneurons (Fig. 1*A–C*). Somewhat surprisingly, however, we also found no overlap of the nonpeptidergic IB4-binding terminals and the PKCγ interneurons in the mouse (Fig. 1*G–I*) and very little overlap in the rat (Fig. 1*D–F*). Instead, there was a distinct segregation, with the IB4-positive terminals located just dorsal to the band of PKCγ interneurons in the mouse (Fig. 1*G–I*). This observation indicates that, if the inner lamina II designation is to be retained, then lamina IIi must be subdivided into dorsal and ventral components (Zylka et al., 2005).

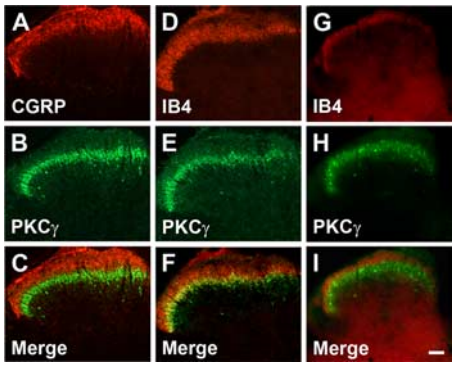

Figure 1. Central termination of the peptidergic and nonpeptidergic afferents in the mouse and rat and their relationship to the PKCγ interneurons of inner lamina II. ***A–C***, CGRP-immunoreactive afferents (***A***) terminate dorsal to the PKCγ-positive neurons (***B***, ***C***). ***D***, Nonpeptidergic afferents, labeled with the IB4 lectin, also terminate mainly dorsal to the PKCγ interneurons. ***E***, ***F***, In the rat, there is some overlap with the PKCγ neurons. ***G–I***, In contrast, in the mouse, there is no overlap between the IB4 terminals (***G***) and PKCγ-immunoreactive neurons (***H***, ***I***). Scale bar, 50 μm.

Transganglionic labeling with WGA or CTB: relationship to the PKCγ interneurons

Studies with the transganglionic tracer WGA, which is carried almost exclusively by small-diameter, unmyelinated afferents (LaMotte et al., 1991), provided further confirmation of the absence of an IB4 projection to the PKCγ interneurons. After injection of WGA into the sciatic nerve of the mouse and rat, we observed very dense labeling in the superficial dorsal horn, laminae I and II. In the mouse, we found that all of the labeling occurred just dorsal to the band of PKCγ interneurons. In the rat, there was limited overlap (see supplemental Fig. 1, available at www.jneurosci.org as supplemental material). In contrast, we found a complementary pattern of transneuronal labeling (i.e., overlap with the PKCγ interneurons) after sciatic nerve injection of CTB, a transganglionic tracer that binds to a surface ganglioside found on medium- and large-diameter dorsal root ganglion neurons with myelinated fibers (Cuatrecasas, 1973; Robertson and Grant, 1985). In sections double stained for CTB (black peroxidase reaction product) and PKCγ (brown product), we found occasional CTB-immunoreactive terminals that were closely apposed to the cell bodies or dendrites of PKCγ interneurons (Fig. 2). Together, the results after transganglionic transport of WGA and CTB indicate that in the mouse, primary afferent (i.e., transneuronally labeled) terminals in the band of PKCγ interneurons arise from myelinated, not from unmyelinated, axons.

We attempted to confirm at the ultrastructural level that PKCγ interneurons received synapses from primary afferents that had transported CTB conjugated to HRP. We found occasional CTB-HRP-labeled terminals that directly apposed PKCγ-immunoreactive interneurons without intervening glial processes (data not shown). However, at the EM level, we never observed a contact that showed a convincing postsynaptic density and clustering of vesicles presynaptically. This finding probably reflected the scarcity of close appositions made by afferent terminals transganglionically labeled with CTB onto PKCγ interneurons that we found at the light microscope level as well as the inherent variability involved in the injection and axonal uptake of any neuronal tracer. Because conclusive identification of morphologically identifiable synapses between afferents labeled with CTB-HRP and PKCγ interneurons would have required an exhaustive and very time-consuming analysis of serial ultrathin sec-

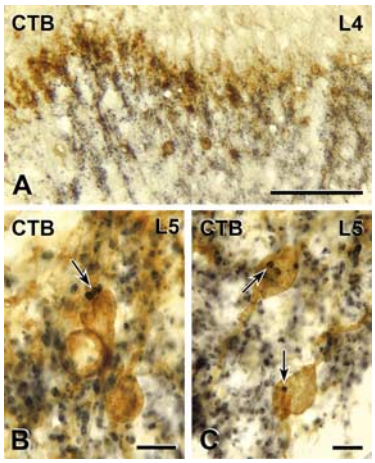

Figure 2. Myelinated primary afferent terminations in the rat and their relationship to the distribution of PKCγ interneurons of inner lamina II. ***A–C***, Transganglionic transport of CTB (black) reveals dense termination in the neck of the dorsal horn, laminae III and IV as well as IIi, which includes the dense band of PKCγ-immunoreactive neurons (brown; ***A***). Some of the CTB-labeled terminals form close appositions (arrows) on PKCγ-immunoreactive cell bodies (brown) in lamina IIi (***B***, ***C***). Scale bars: ***A***, 100 μm; ***B***, ***C***, 10 μm.

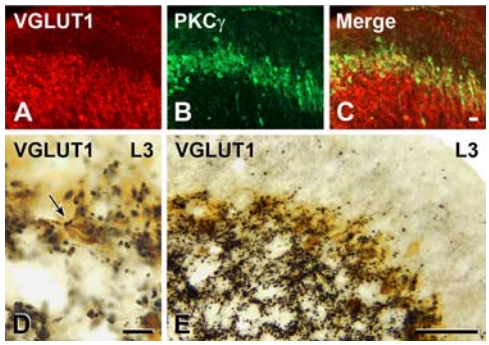

Figure 3. Myelinated primary afferents that express VGLUT1 (in the rat) terminate among PKCγ interneurons. ***A–C***, VGLUT1-immunoreactive axons occur in the layer containing PKCγ-immunoreactive interneurons (yellow; ***C***). ***D***, Two VGLUT1-immunoreactive terminals (arrow) form close appositions on the cell body of a PKCγ-immunoreactive neuron (brown) that lies within the dense band of PKCγ neurons in lamina IIi (taken from the L3 segment). ***E***, In segment L3 as in other spinal segments, the dense band of PKCγ neurons in lamina IIi is heavily innervated by VGLUT1-immunoreactive axons. Scale bars: ***A–C*** (in ***C***), ***D***, 10 μm; *D*, 10 μm; ***E***, 50 μm.

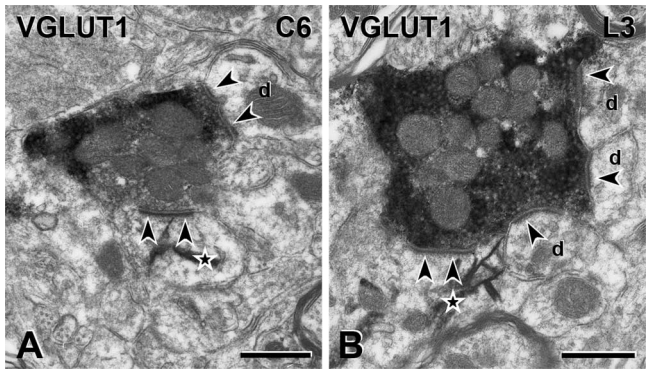

Figure 4. VGLUT1 terminals in the rat are presynaptic to PKCγ interneurons. ***A***, ***B***, VGLUT1-immunoreactive axon terminals form synapses (arrowheads) onto the dendrites of some PKCγ neurons in the dorsal horn of spinal cord segments C6 (***A***) and L3 (***B***). VGLUT1 immunoreactivity is denoted by the amorphous electron-dense peroxidase reaction product and PKCγ immunoreactivity by the presence of TMB-tungstate crystals (stars). Unlabeled dendrites (d), as well as a PKCγ-immunoreactive dendrite, receive synapses (arrowheads) from each VGLUT1 terminal. Scale bars, 500 nm.

tions, we chose to pursue another option for studying myelinated afferent inputs to PKCγ interneurons at the EM level.

VGLUT1 terminals contact PKCγ interneurons in the spinal cord

Because the CTB analysis suggested that there is a myelinated afferent input to IIi and specifically to the PKCγ interneurons, we sought a marker that would not depend on transganglionic transport of CTB-based tracers. Glutamate is the major excitatory neurotransmitter of primary afferents, and antisera directed against VGLUT1, the vesicular glutamate transporter that is associated with large-diameter afferents, immunostain laminae III and IV, consistent with the regions receiving non-nociceptive myelinated afferent input (Oliveira et al., 2003; Landry et al., 2004; Brumovsky et al., 2007). To determine specifically whether PKCγ interneurons are postsynaptic to the VGLUT1-immunoreactive terminals arising from myelinated afferents, we double labeled spinal cord sections with antibodies against PKCγ and VGLUT1.

Both double-immunofluorescence and double-immunoperoxidase staining showed that there is a significant overlap between the distributions of neurons immunoreactive for PKCγ and axons immunoreactive for VGLUT1 (Fig. 3). In lamina II, in peroxidase-stained sections, we were also able to identify close appositions between PKCγ interneurons and VGLUT1-immunoreactive terminals (Fig. 3*D*,*E*). These appositions were much more frequent than the appositions that we found between CTB- or CTB-HRP-labeled afferents and PKCγ interneurons. The relative frequency of VGLUT1 appositions onto PKCγ interneurons compared with CTB appositions led us to extend our light microscopic double-labeling studies to the EM level. We used an amorphous diaminobenzidine reaction product to label VGLUT1-containing terminals and a crystalline tetramethylbenzidine product to identify PKCγ interneurons. As at the light microscope level, we found that lamina IIi contained a host of VGLUT1-immunoreactive terminals in the neuropil between the cell bodies and dendrites of PKCγ interneurons. On a number of occasions, we observed VGLUT1-immunoreactive terminals forming classical asymmetric synapses on PKCγ-immunoreactive dendrites (Fig. 4). In several of these cases, the VGLUT1 terminal also formed synapses on one or more small nonimmunoreactive dendrites, an arrangement that is typical of synaptic glomeruli containing primary afferent terminals in lamina II. The presence of these VGLUT1-immunoreactive synapses strongly suggests that PKCγ interneurons receive a synaptic input from primary afferents with myelinated axons.

Genetic expression of WGA in myelinated sensory neurons of the mouse results in transneuronal labeling of spinal PKCγ interneurons

To confirm that PKCγ interneurons of lamina IIi indeed receive a myelinated input from DRG neurons, we targeted the expression of the transneuronal tracer WGA in myelinated sensory neurons. In these experiments, we used the genetic ZW mouse approach that we recently described (Braz et al., 2002), in which neuronal expression of WGA can be induced in any region of the CNS, after Cre recombination. By following the transneuronal transport of WGA, it is possible to label multisynaptic pathways over long distances (Braz et al., 2005; Braz and Basbaum, 2008). For this study, we used a ZW mouse line (called ZW2) in which there is preferential expression of the inducible tracer in

medium-to-large sensory neurons, because of a fortuitous insertion of the transgene [a detailed characterization of this new transgenic line is in preparation (Braz, unpublished work)]. To induce the expression of WGA in myelinated primary afferent neurons, we crossed ZW2 mice with others that express the Cre recombinase under the control of the NPY promoter (NPY-Cre) (DeFalco et al., 2001). We chose NPY-Cre mice because NPY expression is strongly induced in myelinated DRG neurons after peripheral axotomy (Wakisaka et al., 1991; Noguchi et al., 1993).

In the absence of injury, which includes the side contralateral to the sciatic nerve transection, WGA is expressed, if at all, at very low levels in DRG neurons (Fig. 5*A*). However, 5 d after axotomy, there is a pronounced induction of WGA expression in DRG neurons, ipsilateral to the injury (Fig. 5*B*). The vast majority of WGA-expressing DRG neurons (~90%) were medium to large sized and N52 positive, indicating that they have myelinated axons (Fig. 5*C*). Furthermore, double-labeling experiments indicated that the WGA-expressing DRG neurons also immunostained for NPY and the activating transcription factor ATF-3 (data not shown), which marks axotomized neurons (Tsujino et al., 2000). These latter results confirm that WGA induction resulted from a Cre-mediated recombination event that occurred in axotomized, NPY-positive neurons.

One week after sciatic nerve transection, we observed a dense pattern of WGA-positive terminals in the spinal cord, ipsilateral to the side of the transection, and exclusively in lumbar segments (L2–L6) (Fig. 5*D*). The WGA-immunoreactive terminals were concentrated in the medial regions of the deep laminae of the dorsal horn (III–V), as well as in the ventral horn, which is entirely consistent with the central projection of myelinated DRG neurons at lumbar levels. Transneuronally labeled neurons were also found in laminae III–V. Of particular relevance to the present study, however, we also found that a significant number of PKCγ interneurons in lamina IIi contained the WGA tracer (Fig. 5*E*,*F*). Together with our EM analysis, these genetic tracing results indicate that PKCγ interneurons receive primary afferent inputs from DRG neurons with myelinated axons.

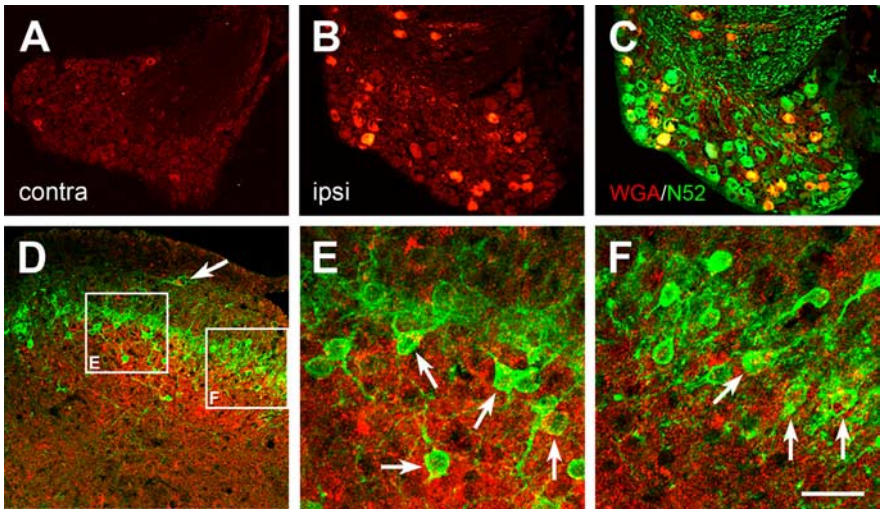

Figure 5. Nerve-injury-triggered expression of the transneuronal tracer WGA in myelinated sensory neurons of the mouse results in transneuronal labeling of spinal PKCγ interneurons. ***A***, Before injury, WGA (red) is expressed at very low levels in DRG neurons of the ZW2 transgenic mouse. ***B***, Axotomy induces expression of WGA in large number of sensory neurons, ipsilateral to the injury. ***C***, Most of the WGA-immunoreactive neurons are myelinated (i.e., are N52 positive; yellow). ***D***, Consistent with the central projection of myelinated DRG neurons, the WGA-positive terminals (red) are concentrated in the medial regions of the deep laminae of the dorsal horn. However, the WGA immunostaining also overlapped extensively with the band of PKCγ interneurons (green) in lamina IIi. ***E***, ***F***, Higher magnification of the white boxes in ***D*** shows that some of these PKCγ interneurons contain the WGA tracer (arrows), indicating that they are directly postsynaptic to myelinated primary afferent fibers. Note that some of the scattered PKCγ interneurons in both laminae I (arrow in ***D***) and IIi also receive inputs from myelinated sensory neurons. Scale bar: (in ***F***) ***A–D***, 100 μm; ***E***, ***F***, 6.25 μm.

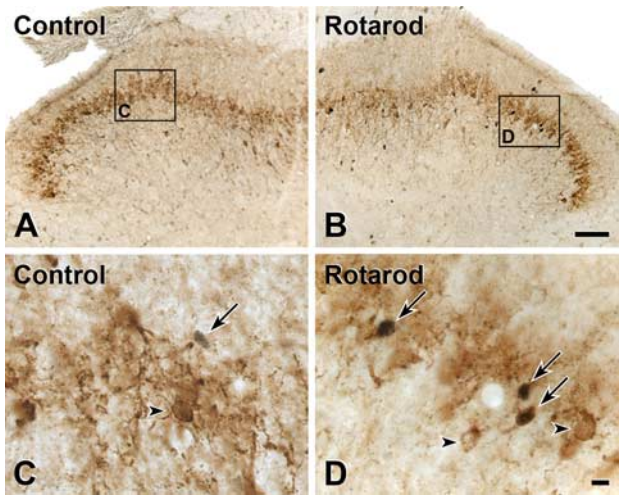

Figure 6. Walking on a rotarod induces Fos expression in PKCγ interneurons of the rat. Double-label immunocytochemistry for Fos (black) and PKCγ (brown) is shown. ***A***, ***B***, The number of Fos-positive neurons in the superficial and deep dorsal horn in mice that walked on the rotating rod (***B***) was significantly greater than the number recorded in mice that rested in their cages (***A***). ***C***, Higher-magnification images demonstrate that there is no overlap between Fos (arrow) and PKCγ-immunoreactive interneurons in control mice (arrowhead). ***D***, There is, however, a significant increase in the number of neurons that double label for Fos and PKCγ in animals that walked on the rotarod (arrows). Note that not all PKCγ-immunoreactive neurons express Fos in the rotarod animals (***D***, arrowheads). Scale bars: (in ***B***) ***A***, ***B***, 50 μm; (in ***D***) ***C***, ***D***, 10 μm.

Walking on a rotarod induces Fos expression in PKCγ interneurons

With a view to assessing the functional significance of the myelinated afferent input to PKCγ interneurons, we used Fos expression to monitor the activity of these neurons. In a previous report in the rat, we found that walking on a rotarod induced significant Fos immunoreactivity in neurons in the inner part of lamina II (Jasmin et al., 1994). Here, we asked whether the Fos expression that we observed in that study included the PKCγ subset of interneurons that populate this region of the cord. We compared the magnitude of Fos expression after 90 min of continuous walking on a rotating rod ($n = 4$) to that observed in naive animals that rested in their cages ($n = 3$). As we previously reported, there is minimal Fos expression in control rats (Fig. 6*A*,*C*). However, there was a marked increase in the number of Fos-immunoreactive neurons in inner lamina II, and in the number of neurons double labeled for PKCγ and Fos in rats that walked on the rotating rod (Fig. 6*B*,*D*). In the control group, only 4.6% of Fos neurons in lamina IIi were immunoreactive for PKCγ, whereas 25% were double labeled in the experimental group. The difference was highly significant ($p < 0.001$).

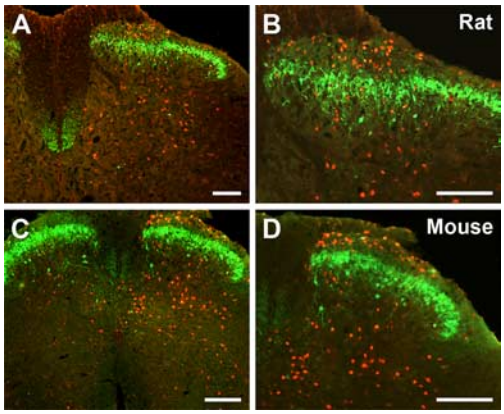

Figure 7. In mouse and rat, noxious stimulation does not induce Fos expression in PKCγ interneurons. Ninety minutes after unilateral injection of formalin to the hindpaw, Fos expression is increased in the spinal cord in both superficial and deep laminae of the spinal cord. ***A***, ***B***, Although we observed a few Fos-immunoreactive neurons in the layer of interneurons that contain PKCγ cells in the rat, we never found double-labeled cells. ***C***, ***D***, In the mouse, all noxious stimulus-evoked Fos immunoreactivity was outside of the PKCγ layer of interneurons. Scale bars, 100 μm.

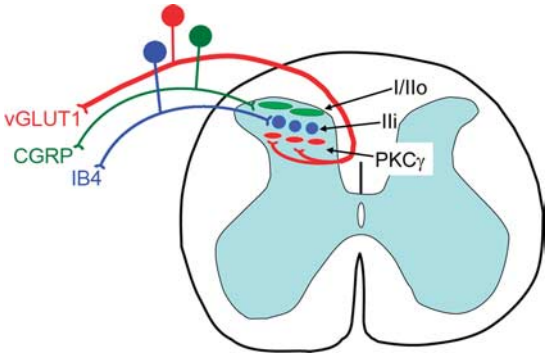

Figure 8. Schematic diagram illustrating the discrete laminar organization of the central projections of unmyelinated and myelinated afferents in the superficial dorsal and their relationship to the band of PKCγ-expressing interneurons. Peptidergic primary afferents denoted by the CGRP (green) population target projection neurons and interneurons in laminae I and outer II. Nonpeptidergic primary afferents, denoted by their binding of IB4 (blue), target neurons just ventral to the CGRP terminal zone, in inner lamina II. The IB4 terminals do not target the PKCγ band of interneurons. Instead, myelinated afferents that express the vesicular glutamate transporter (VGLUT1; red) target and synapse onto the PKCγ interneurons, which are located in the most ventral part of inner lamina II. The current results provide further evidence for the remarkable stratification of the superficial dorsal horn and indicate that non-noxious stimuli conveyed by myelinated fibers provide input to the PKCγ interneurons.

Noxious stimulation does not induce Fos expression in PKCγ interneurons

In marked contrast to the results from innocuous stimulation above, in which double-labeled PKCγ/Fos interneurons were observed in lamina IIi, noxious stimulation by injection of formalin into the hindpaw failed to produce double-labeled PKCγ/Fos interneurons (Fig. 7). This was true for both the mouse and the rat. Compared with the control, uninjected paw, there was a marked increase in the number of Fos expressing neurons (red) in the superficial (laminae I and IIo) and deep (laminae III–V) dorsal horn, but there was no double labeling of PKCγ interneurons (green).

Discussion

In contrast to the prevailing view that the nonpeptide population of primary afferent nociceptors targets the PKCγ interneurons, our studies demonstrate that these interneurons, which have been strongly implicated in the development of injury-induced persistent pain conditions, receive inputs from myelinated afferents. Because we did not find overlap of the IB4-binding unmyelinated afferents with the PKCγ population, it appears that the segregation of the unmyelinated afferents and the PKCγ interneurons is complete in the mouse. In contrast, there is some limited overlap in the rat. Importantly, in the transgenic mouse in which the inducible transneuronal tracer WGA was expressed in DRG neurons with myelinated fibers, we observed that PKCγ interneurons of lamina IIi were transneuronally labeled with WGA. This finding conclusively demonstrates that there is a circuit connecting myelinated primary afferent neurons to PKCγ interneurons. Because the transneuronal labeling was detected in these interneurons within 5 d of sciatic nerve transection, we suggest that these connections are monosynaptic.

We also found that innocuous, but not noxious, stimulation induces Fos expression in the PKCγ interneurons. This observation provides an important functional correlate of the myelinated afferent input to these neurons. Figure 8 highlights the remarkable lamination that characterizes the superficial dorsal horn. Thus, inner lamina II consists of multiple components, with the dorsalmost part receiving inputs from the nonpeptidergic population of afferents, including its $P2X_3$- and MrgD-expressing subsets, and the ventral part receiving inputs from myelinated afferents, at least some of which express the vesicular glutamate transporter, VGLUT1.

Consistent with our conclusion, Zylka et al. (2005) recently reported that neither the IB4 nonpeptidergic population nor the central terminals of the MrgD subset of the IB4 afferents overlapped with the PKCγ interneurons. Most importantly, by following the transneuronal transport of a genetically expressed tracer from a subpopulation of IB4 afferents, our laboratory demonstrated not only that there are no monosynaptic IB4 connections with the PKCγ interneurons, but also that there are not even indirect, polysynaptic connections (Braz et al., 2005). Because we never found transneuronal labeling of the PKCγ interneurons, these cells are unlikely to be part of the central circuits targeted by the nonpeptidergic nociceptors. Somewhat paradoxically, Li et al. (2001) provide examples of SP-PKCγ and IB4-PKCγ synaptic connections; however, those examples were taken from laminae I and IIo. As such, they almost certainly represented inputs to the scattered PKCγ interneurons located outside of the major band of PKCγ interneurons in inner lamina II.

Our results are entirely consistent with previous reports on the failure of noxious stimulation to induce Fos in inner lamina II (Menétrey et al., 1989; Presley et al., 1990), an observation that we now extend by showing that hindpaw formalin injection does not induce Fos expression in PKCγ interneurons (Fig. 7). In contrast, using walking on a rotarod to engage non-nociceptive mechanoreceptors, we not only confirmed that inner lamina II interneurons are activated by innocuous inputs (Woolf and Fitzgerald, 1983) but also showed that a significant number of the activated interneurons are PKCγ positive.

Using markers of myelinated afferents, we further demonstrated that PKCγ interneurons do receive primary afferent input from myelinated fibers. Thus, transganglionic transport of CTB resulted in the labeling of afferent terminals that overlapped with the PKCγ interneurons. Because we did not find CTB-labeled afferents dorsal to the band of PKCγ interneurons, it is almost certain that this input arises from afferents

that enter from below, i.e., from lamina III of the dorsal horn (Fig. 2*A*). These terminals presumably arise from the dorsalmost extensions of arbors that have been described in Golgi studies (Scheibel and Scheibel, 1969; Beal and Fox, 1976; Beal, 1979; Beal et al., 1988; Ramón y Cajal, 1904) and in studies examining the arborization of intracellularly filled single afferent fibers (Light and Perl, 1979; Woolf, 1987; Shortland et al., 1989; Shortland and Woolf, 1993). Because we found CTB-HRP-containing terminals that directly apposed PKCγ without intervening glial processes, we are confident that a more extensive search would have revealed synapses by CTB-HRP-labeled terminals onto PKCγ interneurons. In fact, in previous work we demonstrated that approximately one-half the terminals that appear to closely appose a neuron at the light microscope level actually form synapses at the EM level (Pilowsky et al., 1992). We also established that axons immunoreactive for VGLUT1, which marks myelinated afferents (Alvarez et al., 2004), overlapped with the PKCγ interneurons. Furthermore, we showed at the ultrastructural level that VGLUT1-containing axons synapse onto PKCγ interneurons, confirming a direct synaptic input. Finally, we demonstrated that triggering expression of WGA in myelinated afferents, but not in the IB4-binding population of unmyelinated afferents (Braz et al., 2005), results in its transneuronal transport to the PKCγ interneurons (Fig. 5).

Our anatomical analysis was not able to unequivocally determine the modality of the myelinated fiber input. Nevertheless, the fact that walking on a rotarod, but not noxious stimulation, induces Fos in the PKCγ interneurons argues that innocuous stimuli activate these interneurons. We suggest, therefore, that the myelinated afferents are non-nociceptive, probably either low-threshold Aδ afferents that innervate D hairs or Aβ afferents. Consistent with this proposal, several groups (Trevino et al., 1972; Bennett et al., 1980; Woolf and Fitzgerald, 1983) have reported that neurons in the inner part of lamina II are largely responsive to innocuous stimulation, in contrast to the nociresponsive neurons located more dorsally. We recognize that there may be inputs from low-threshold unmyelinated afferents to the PKCγ layer of interneurons (Light and Perl, 2003), perhaps from muscle (Ling et al., 2003), but these likely correspond to a rather limited population that is neither peptidergic nor binds IB4.

How does a myelinated input to PKCγ interneurons contribute to nerve injury-induced mechanical allodynia?

If the output circuit for producing pain is not altered after injury, there could be several conditions through which non-nociceptive myelinated afferents that normally innervate PKCγ interneurons could induce pain in the setting of injury. First, excitability of these circuits may be increased secondary to the injury, presumably via C fiber input-induced central sensitization (Cook et al., 1987; Hylden et al., 1989; Woolf and King, 1990; Simone et al., 1991; Grubb et al., 1993). Second, supraspinal inhibitory control of these circuits may be decreased or facilitatory control increased (Schaible et al., 1991; Dubner and Ren, 2004). Third, there may be anatomical reorganization of the afferent fibers so that innocuous inputs carried by myelinated afferents engage "pain" transmission circuits with which they are not normally connected.

If the excitability of the PKCγ interneuron is indeed enhanced in the setting of injury, and if the PKCγ interneuron engages "pain" transmission circuits, then innocuous inputs carried by myelinated afferents could drive pain behavior. This is presumably a natural response to injury, leading to protection of the injured body part. Furthermore, if in the setting of injury, PKCγ is critical to the excitability changes that occur in downstream "pain" transmission circuits, then its deletion would reduce the likelihood that innocuous inputs produce pain after injury. This is precisely what we found in PKCγ mutant mice (Malmberg et al., 1997).

Conceivably, any or all of the many other mechanisms that have been implicated in injury-induced increases in the excitability of dorsal horn nociresponsive neurons may involve PKCγ interneurons. Indeed, Miraucourt et al. (2007) recently provided evidence that PKCγ neurons are part of a local circuit that mediates dynamic mechanical allodynia after loss of glycinergic inhibitory control. Interestingly, ketamine injection into the rostral ventral medulla, even in the absence of injury, induces Fos expression in interneurons of inner lamina II (Bett and Sandkühler, 1995). Although the neurochemistry of the Fos-positive neurons was not identified, it is reasonable to hypothesize that the PKCγ interneurons are involved and that increased descending facilitation, which occurs in the setting of injury (Vera-Portocarrero et al., 2006), activated these neurons.

What is the target of the PKCγ interneuron?

The PKCγ interneurons are a subset of islet cells that populates inner lamina II. Because both the dendrites and axons of all islet cells arborize within lamina IIi (Gobel, 1978), it is likely that their targets include other lamina IIi interneurons, as well as other PKCγ interneurons. In fact, we found PKCγ-immunoreactive terminals synapsing onto PKCγ-immunoreactive somata. It is also possible that these interneurons target the few dorsally located lamina II interneurons that have dendrites that penetrate inner lamina II (e.g., stalked cells) or the neurons located in the deeper dorsal horn that have dendrites that arborize dorsally into the superficial dorsal horn (Brown et al., 1977; Brown, 1981). Our ongoing studies are targeting these questions, using techniques that allow for the selective induction of anterograde tracers in the PKCγ interneurons.

In summary, our results demonstrate that myelinated rather than unmyelinated fibers provide the predominant input to PKCγ interneurons, which have previously been reported to be involved in the development of persistent pain after tissue or nerve injury (Malmberg et al., 1997). Our current observations provide a novel perspective on the mechanisms through which injury engages the PKCγ interneurons to produce mechanical hypersensitivity. We suggest that this condition results from enhanced signaling by myelinated afferents that normally innervate these neurons. Thus, injury-induced alterations in sensory processing probably occur within a circuit that contains primary myelinated fibers, PKCγ interneurons, and the dorsal horn output neurons.

References

Alvarez FJ, Villalba RM, Zerda R, Schneider SP (2004) Vesicular glutamate transporters in the spinal cord, with special reference to sensory primary afferent synapses. J Comp Neurol 472:257–280.

Beal JA (1979) Serial reconstruction of Ramon y Cajal's large primary afferent complexes in laminae II and III of the adult monkey spinal cord: a Golgi study. Brain Res 166:161–165.

Beal JA, Fox CA (1976) Afferent fibers in the substantia gelatinosa of the adult monkey (*Macaca mulatta*): a Golgi study. J Comp Neurol 168:113–143.

Beal JA, Russell CT, Knight DS (1988) Morphological and developmental characterization of local-circuit neurons in lamina III of the rat spinal cord. Neurosci Lett 86:1–5.

Bennett GJ, Abdelmoumene M, Hayashi H, Dubner R (1980) Physiology and morphology of substantia gelatinosa neurons intracellularly stained with horseradish peroxidase. J Comp Neurol 194:809–827.

Bett K, Sandkühler J (1995) Map of spinal neurons activated by chemical stimulation in the nucleus raphe magnus of the unanesthetized rat. Neuroscience 67:497–504.

Braz JM, Basbaum AI (2008) Genetically expressed transneuronal tracer reveals direct and indirect serotonergic descending control circuits. J Comp Neurol 507:1990–2003.

Braz JM, Rico B, Basbaum AI (2002) Transneuronal tracing of diverse CNS circuits by Cre-mediated induction of wheat germ agglutinin in transgenic mice. Proc Natl Acad Sci U S A 99:15148–15153.

Braz JM, Nassar MA, Wood JN, Basbaum AI (2005) Parallel "pain" pathways arise from subpopulations of primary afferent nociceptor. Neuron 47:787–793.

Brown A (1981) Organization of the spinal cord. New York: Springer.

Brown AG, Rose PK, Snow PJ (1977) The morphology of hair follicle afferent fibre collaterals in the spinal cord of the cat. J Physiol 272:779–797.

Brumovsky P, Watanabe M, Hökfelt T (2007) Expression of the vesicular glutamate transporters-1 and -2 in adult mouse dorsal root ganglia and spinal cord and their regulation by nerve injury. Neuroscience 147:469–490.

Cook AJ, Woolf CJ, Wall PD, McMahon SB (1987) Dynamic receptive field plasticity in rat spinal cord dorsal horn following C-primary afferent input. Nature 325:151–153.

Cuatrecasas P (1973) Interaction of *Vibrio cholerae* enterotoxin with cell membranes. Biochemistry 12:3547–3558.

DeFalco J, Tomishima M, Liu H, Zhao C, Cai X, Marth JD, Enquist L, Friedman JM (2001) Virus-assisted mapping of neural inputs to a feeding center in the hypothalamus. Science 291:2608–2613.

Dubner R, Ren K (2004) Brainstem mechanisms of persistent pain following injury. J Orofac Pain 18:299–305.

Gobel S (1978) Golgi studies of the neurons in layer II of the dorsal horn of the medulla (trigeminal nucleus caudalis). J Comp Neurol 180:395–413.

Grubb BD, Stiller RU, Schaible HG (1993) Dynamic changes in the receptive field properties of spinal cord neurons with ankle input in rats with chronic unilateral inflammation in the ankle region. Exp Brain Res 92:441–452.

Hsu SM, Raine L, Fanger H (1981) The use of antiavidin antibody and avidin-biotin-peroxidase complex in immunoperoxidase technics. Am J Clin Pathol 75:816–821.

Hunt SP, Mantyh PW (2001) The molecular dynamics of pain control. Nat Rev Neurosci 2:83–91.

Hylden JL, Nahin RL, Traub RJ, Dubner R (1989) Expansion of receptive of spinal lamina I projection neurons in rats with unilateral adjuvant-induced inflammation: the contribution of dorsal horn mechanisms. Pain 37:229–243.

Jasmin L, Gogas KR, Ahlgren SC, Levine JD, Basbaum AI (1994) Walking evokes a distinctive pattern of Fos-like immunoreactivity in the caudal brainstem and spinal cord of the rat. Neuroscience 58:275–286.

LaMotte CC, Kapadia SE, Shapiro CM (1991) Central projections of the sciatic, saphenous, median, and ulnar nerves of the rat demonstrated by transganglionic transport of choleragenoid-HRP (B-HRP) and wheat germ agglutinin-HRP (WGA-HRP). J Comp Neurol 311:546–562.

Landry M, Bouali-Benazzouz R, El Mestikawy S, Ravassard P, Nagy F (2004) Expression of vesicular glutamate transporters in rat lumbar spinal cord, with a note on dorsal root ganglia. J Comp Neurol 468:380–394.

Li JL, Li YQ, Nomura S, Kaneko T, Mizuno N (2001) Protein kinase C gamma-like immunoreactivity in the substantia gelatinosa of the medullary dorsal horn of the rat. Neurosci Lett 311:185–188.

Light AR, Perl ER (1979) Spinal termination of functionally identified primary afferent neurons with slowly conducting myelinated fibers. J Comp Neurol 186:133–150.

Light AR, Perl ER (2003) Unmyelinated afferents are not just for pain anymore. J Comp Neurol 461 2137–139.

Ling LJ, Honda T, Shimada Y, Ozaki N, Shiraishi Y, Sugiura Y (2003) Central projection of unmyelinated (C) primary afferent fibers from gastrocnemius muscle in the guinea pig. J Comp Neurol 461:140–150.

Llewellyn-Smith IJ, Minson JB (1992) Complete penetration of antibodies into vibratome sections after glutaraldehyde fixation and ethanol treatment: light and electron microscopy for neuropeptides. J Histochem Cytochem 40:1741–1749.

Llewellyn-Smith IJ, Pilowsky P, Minson JB (1993) The tungstate-stabilized tetramethylbenzidine reaction for light and electron microscopic immunocytochemistry and for revealing biocytin-filled neurons. J Neurosci Methods 46:27–40.

Llewellyn-Smith IJ, Dicarlo SE, Collins HL, Keast JR (2005) Enkephalin-immunoreactive interneurons extensively innervate sympathetic preganglionic neurons regulating the pelvic viscera. J Comp Neurol 488:278–289.

Llewellyn-Smith IJ, Martin CL, Fenwick NM, Dicarlo SE, Lujan HL, Schreihofer AM (2007) VGLUT1 and VGLUT2 innervation in autonomic regions of intact and transected rat spinal cord. J Comp Neurol 503:741–767.

Malmberg AB, Chen C, Tonegawa S, Basbaum AI (1997) Preserved acute pain and reduced neuropathic pain in mice lacking PKCγ. Science 278:279–283.

McNeill DL, Chung K, Carlton SM, Coggeshall RE (1988) Calcitonin gene-related peptide immunostained axons provide evidence for fine primary afferent fibers in the dorsal and dorsolateral funiculi of the rat spinal cord. J Comp Neurol 272:303–308.

Menétrey D, Gannon A, Levine JD, Basbaum AI (1989) Expression of c-fos protein in interneurons and projection neurons of the rat spinal cord in response to noxious somatic, articular, and visceral stimulation. J Comp Neurol 285:177–195.

Miraucourt LS, Dallel R, Voisin DL (2007) Glycine inhibitory dysfunction turns touch into pain through PKCγ interneurons. PLoS ONE 2:e1116.

Mori M, Kose A, Tsujino T, Tanaka C (1990) Immunocytochemical localization of protein kinase C subspecies in the rat spinal cord: light and electron microscopic study. J Comp Neurol 299:167–177.

Noguchi K, De León M, Nahin RL, Senba E, Ruda MA (1993) Quantification of axotomy-induced alteration of neuropeptide mRNAs in dorsal root ganglion neurons with special reference to neuropeptide Y mRNA and the effects of neonatal capsaicin treatment. J Neurosci Res 35:54–66.

Oliveira AL, Hydling F, Olsson E, Shi T, Edwards RH, Fujiyama F, Kaneko T, Hökfelt T, Cullheim S, Meister B (2003) Cellular localization of three vesicular glutamate transporter mRNAs and proteins in rat spinal cord and dorsal root ganglia. Synapse 50:117–129.

Pilowsky P, Llewellyn-Smith IJ, Lipski J, Chalmers J (1992) Substance P immunoreactive boutons form synapses with feline sympathetic preganglionic neurons. J Comp Neurol 320:121–135.

Polgár E, Fowler JH, McGill MM, Todd AJ (1999) The types of neuron which contain protein kinase C gamma in rat spinal cord. Brain Res 833:71–80.

Presley RW, Menétrey D, Levine JD, Basbaum AI (1990) Systemic morphine suppresses noxious stimulus-evoked Fos protein-like immunoreactivity in the rat spinal cord. J Neurosci 10:323–335.

Ramón y Cajal S (1904) Histology of the nervous system. Reprint (Swanson N, Swanson L, translators). New York: Oxford UP, 1995.

Robertson B, Grant G (1985) A comparison between wheat germ agglutinin-and choleragenoid-horseradish peroxidase as anterogradely transported markers in central branches of primary sensory neurones in the rat with some observations in the cat. Neuroscience 14:895–905.

Schaible HG, Neugebauer V, Cervero F, Schmidt RF (1991) Changes in tonic descending inhibition of spinal neurons with articular input during the development of acute arthritis in the cat. J Neurophysiol 66:1021–1032.

Scheibel ME, Scheibel AB (1969) Terminal patterns in cat spinal cord. 3. Primary afferent collaterals. Brain Res 13:417–443.

Shortland P, Woolf CJ (1993) Morphology and somatotopy of the central arborizations of rapidly adapting glabrous skin afferents in the rat lumbar spinal cord. J Comp Neurol 329:491–511.

Shortland P, Woolf CJ, Fitzgerald M (1989) Morphology and somatotopic organization of the central terminals of hindlimb hair follicle afferents in the rat lumbar spinal cord. J Comp Neurol 289:416–433.

Silverman JD, Kruger L (1990) Selective neuronal glycoconjugate expression in sensory and autonomic ganglia: relation of lectin reactivity to peptide and enzyme markers. J Neurocytol 19:789–801.

Simone DA, Sorkin LS, Oh U, Chung JM, Owens C, LaMotte RH, Willis WD (1991) Neurogenic hyperalgesia: central neural correlates in responses of spinothalamic tract neurons. J Neurophysiol 66:228–246.

Snider WD, McMahon SB (1998) Tackling pain at the source: new ideas about nociceptors. Neuron 20:629–632.

Trevino DL, Maunz RA, Bryan RN, Willis WD (1972) Location of cells of origin of the spinothalamic tract in the lumbar enlargement of cat. Exp Neurol 34:64–77.

Tsujino H, Kondo E, Fukuoka T, Dai Y, Tokunaga A, Miki K, Yonenobu K, Ochi T, Noguchi K (2000) Activating transcription factor 3 (ATF3) induction by axotomy in sensory and motoneurons: a novel neuronal marker of nerve injury. Mol Cell Neurosci 15:170–182.

Vera-Portocarrero LP, Zhang ET, Ossipov MH, Xie JY, King T, Lai J, Porreca F (2006) Descending facilitation from the rostral ventromedial medulla maintains nerve injury-induced central sensitization. Neuroscience 140:1311–1320.

Wakisaka S, Kajander KC, Bennett GJ (1991) Increased neuropeptide Y (NPY)-like immunoreactivity in rat sensory neurons following peripheral axotomy. Neurosci Lett 124:200–203.

Woolf CJ (1987) Central terminations of cutaneous mechanoreceptive afferents in the rat lumbar spinal cord. J Comp Neurol 261:105–119.

Woolf CJ, Fitzgerald M (1983) The properties of neurones recorded in the superficial dorsal horn of the rat spinal cord. J Comp Neurol 221:313–328.

Woolf CJ, King AE (1990) Dynamic alterations in the cutaneous mechanoreceptive of dorsal horn neurons in the rat spinal cord. J Neurosci 10:2717–2726.

Zylka MJ, Rice FL, Anderson DJ (2005) Topographically distinct epidermal nociceptive circuits revealed by axonal tracers targeted to Mrgprd. Neuron 45:17–25.